

Optimization of Pulsating Blank Holder Force for Deep Drawing of Cylindrical Cups

Jing Han¹, Shinji Natsume², Satoshi Kitayama², Koetsu Yamazaki², Hiroaki Uchida¹

¹ Universal Can Corporation, Sunto, Japan, hanjing@mmc.co.jp

² Kanazawa University, Kanazawa, Japan

1. Abstract

A further improvement in the drawability may lead to a further light-weight cylindrical drawn cup, hence to a more environment-friendly and sustainable industrial product such as an aluminium beverage can & bottle. A pulsating blank holder force (BHF) with a frequency ranged from ultra-high to ultra-low values, is reported that can improve the drawability, as compared with a static constant BHF. However, it still needs a lot of efforts before applying the pulsating BHF industrially, for example, investigation into the optimum property of vibration added to the blank holder during deep drawing of cylindrical cups.

This study implemented an optimization on the properties of the vibration such as the oscillation amplitude, frequency and phase, by applying the structure optimization technique, based on numerical simulations of the cup drawing process. Parameters used to determine a sinusoidal vibration wave are taken as design variables. Wrinkling and tearing are major defects in deep drawing, therefore are considered as design constraints. The limit drawing ratio (LDR) is one of indicators to evaluate the drawability, therefore LDR is maximized through maximizing the limiting drawing depth that could be achieved for a specified drawing ratio. A sequential approximate optimization method is successfully applied to perform design optimization, which leading to a satisfied improvement in the drawability.

2. Keywords: Deep drawing process, Formability, Cylindrical cup, Pulsating blank holder force, Optimum design.

3. Introduction

As shown in [Figure 1](#), during deep drawing of a cylindrical cup, the circular punch forces the blank through the draw die and forms into a cup. The blank holder is used to prevent it from wrinkling due to the tangential compressive strain in the forming zone. The limit drawing ratio (LDR), defined as the ratio of the maximum blank diameter which is successfully drawn to the punch diameter, is one of indicators to evaluate the drawability. Factors causing wrinkling, tearing and earring during deep drawing, such as material properties and shape dimensions of the blank / tools, lubrication condition between the blank and tools, temperature and forming speed, have been extensively studied experimentally, theoretically and numerically [1-10].

A further improvement in the sheet formability may lead to a further light-weight cylindrical drawn cup, hence to a more environment-friendly and sustainable industrial product, for example, an aluminium beverage can & bottle ([Figure 2](#)) [11]. To improve formability and forming quality, a lot of techniques have been investigated, for example, groove pressing the blank, coating the tools, shaping the surfaces of the blank holder, adding lubrication holes on the die shoulder, applying an adaptive blank holder force (BHF) varying with the punch stroke, and applying a circumferentially segmented BHF [12-18]. Moreover, forming processes with hydraulic pressure [19-21], with high-pressured water jet [22], with a radial inward force in the flange region [23], are also being developed.

Recently, a pulsating BHF with a frequency ranged from ultra-high to ultra-low values is reported that can reduce friction and deformation resistance, hence can increase LDR, as compared with a static constant BHF [24-27]. With industrial technology fast developing, practicality of the pulsating BHF may be expected. However, it still needs a lot of efforts before applying the pulsating BHF industrially, for example, investigation into the optimum property of vibration added to the blank holder during deep drawing of cylindrical cups.

On the other hand, research and development of the structural optimization technique and its applications on the metal sheet forming process have been going on. The response surface approximation method is one of practical optimization methods, therefore is applied widely in industry. To efficiently obtain accurate response surfaces, the orthogonal array in the design-of-experiment technique is used [28]. Recently, several new techniques have been proposed and applied to improve accuracy of the approximation. The sequential approximate optimization (SAO) method using radial basis function (RBF) network has been applied to

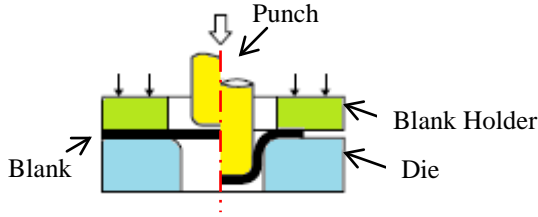


Figure 1: Deep drawing of cylindrical cups



Figure 2: An aluminium beverage bottle

optimize a series of sheet metal forming processes, for efficiently searching a highly accurate global optimal solution [29-31].

This study optimizes the properties of the vibration such as the amplitude, frequency and phase, based on deep drawing simulations. Parameters used to determine a sinusoidal vibration wave are taken as design variables. Wrinkling and tearing are considered as design constraints. LDR is maximized through maximizing the limiting drawing depth that could be achieved for a specified larger drawing ratio. The SAO method using RBF network is applied to perform design optimization.

4. Deep drawing process simulation

A three-dimensional finite element analysis model is established to simulate deep drawing process of the cylindrical cup with the static constant BHF and with various pulsating BHF.

4.1. Finite element model

Figure 3 shows the deep drawing analysis model used in this study [18]. The flat circular blank is clamped by the circular die ring and the blank holder with smooth surfaces. In order to save calculating cost, one-fourth finite element model is adopted due to symmetry. The explicit finite element code, LS-DYNA is utilized to perform the deep drawing simulation.

The blank with 83.44mm diameter and 0.208mm initial uniform thickness t_0 , is divided by four-node shell elements. The aluminium blank is defined as an elasto-plastic body, and the material properties are assumed as Young's modulus: 68.9GPa, Poisson's ratio: 0.33.

The diameter of the punch is 45.72 mm; hence, the draw ratio comes to be 1.8, which is larger than usual. The punch moves at a constant speed of $v_0 = 350$ mm/s. The diameter of the die is 46.74 mm. Both the die and blank holder are defined as rigid bodies. The friction coefficient between tools and the blank is assumed as 0.05.

The pulsating BHF used in this study is defined in Eq. (1),

$$PBHF = F_0 + aF_0 \sin(2\pi ft + \phi) \quad (1)$$

Where, F_0 is a primary BHF, f denotes the pulsating frequency, ϕ denotes the phase, and aF_0 represents the amplitude, a is a scalar ranged from 0 to 1, t is punch moving time. Figure 4 shows example sine curves for calculating the pulsating BHF defined by the same parameters of F_0 , a , f but different ϕ .

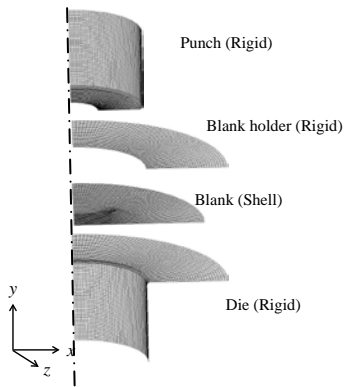


Figure 3 : Numerical analysis model

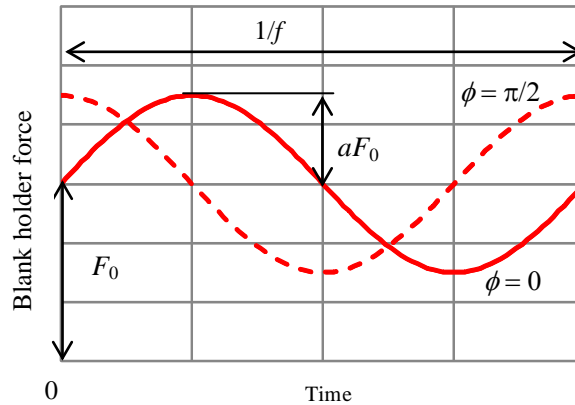


Figure 4: Example curves of pulsating BHF

4.2. Simulation results

In deep drawing process, excessive material flow causes wrinkling at the flange (Figure 5(a)) while insufficient material flow leads to thinning and tearing of the cup (Figure 5(b)). For convenient, the ratio ($r_w = D_{max} / t_0$) of the maximum axial distance D_{max} between the blank holder and the die during the deep drawing process to the initial blank thickness t_0 , is used to predict the risk of wrinkling. The ratio ($r_t = t_{min} / t_0$) of the minimum thickness t_{min} of the cup to the initial blank thickness t_0 , is used to predict the risk of tearing. In this study, defects of the drawn cup are determined when r_w is more than 1.2 or r_t is less than 0.8.

To a given relatively large draw ratio, the limiting drawing depth L_a that can be achieved before wrinkling or tearing occurs, during the deep drawing process, is used as an indicator to compare the drawability.

In order to observe the influences of the parameters of the pulsating BHF on the drawability, deep drawing simulations were carried out for several models with the static constant BHF as well as with various pulsating blank holder force, as shown in Table 1 and Figure 6. Model 1 and Model 2 were applied by the static constant BHF, while else models were applied by the pulsating BHF of various vibration properties defined by Eq.(1) in terms of four parameters. The points at where wrinkling or tearing occurred, are marked with symbols for each model in the same figure, respectively.

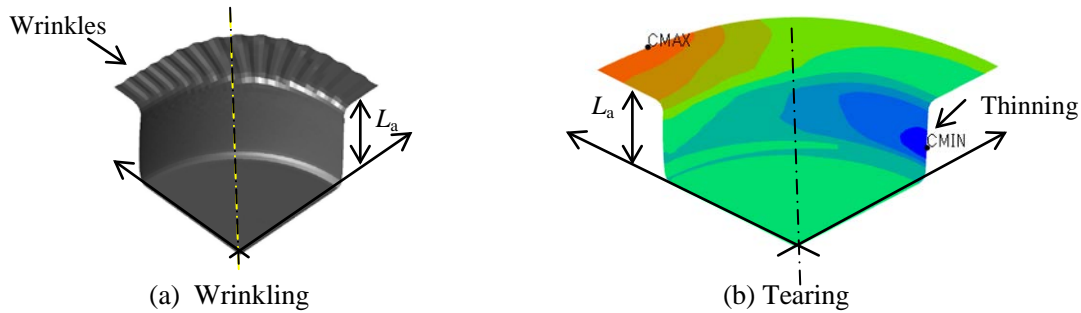


Figure 5: Defects in deep drawing process

Table 1 Finite element analysis results

Model	F_0 / kN	a	f / Hz	ϕ	L_a / mm	Results
1	1.000	N/A	N/A	N/A	12.20	Wrinkling
2	2.000	N/A	N/A	N/A	9.10	Tearing
3	4.786	0.815	5.536	3.899	13.7	Wrinkling
4	2.264	0.332	14.062	4.866	9.45	Tearing
5	0.539	0.768	15.815	3.421	2.45	Wrinkling
6	3.835	0.624	1.249	2.497	4.20	Tearing

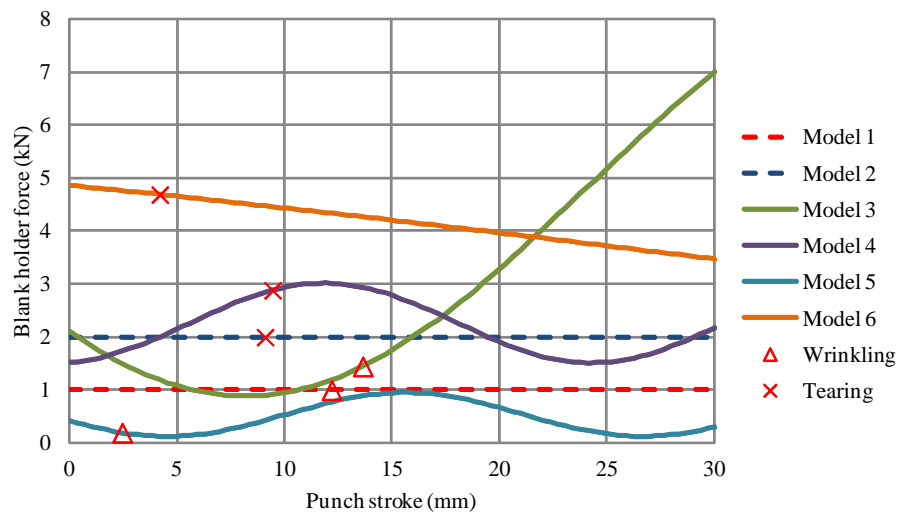


Figure 6: Simulation results of models applied by various BHF

Simulation results, for example, results of Model 1 and Model 2 show that the given blank cannot be drawn successfully into a cup with the given tooling systems. Wrinkling occurs if BHF is too small as that in Model 1, and tearing occurs if BHF is too large as that in Model 2.

Simulation results of Model 3 and Model 4 show that, by applying the pulsating BHF, the limiting drawing depth L_a can be extended, in other words, failure can be delayed, and a deeper cup may be obtained.

However, simulation results of Model 5 and Model 6 show that, by applying the pulsating BHF, the limiting drawing depth L_a also may be shortened, which is not expected.

On the basis of numerical simulation results, it is confirmed that the parameters of the pulsating BHF do influence the deep drawing process, and that need to be investigated and optimized to obtain a drawn cup of a deeper depth, hence, to achieve a larger drawing ratio.

5. Optimization of pulsating BHF

5.1. Formulation of the optimization problem

The parameters of the pulsating BHF are selected as design variables. The objective of the optimization is to maximize the limiting drawing depth L_a for a specific larger drawing ratio. The ratios r_w and r_t are defined as design constraints to avoid wrinkling and tearing. The optimization problem is then posted as

$$\text{Find design variables: } X = \{x_i\}, \quad i = 1, \dots, n \quad (n: \text{the number of design variables}) \quad (2)$$

$$\text{Maximize } f(X) = L_a(X), \quad (3)$$

Subject to

$$g_1 = r_w / r_{w\max} - 1 \leq 0, \quad (4)$$

$$g_2 = r_{t\min} / r_t - 1 \leq 0, \quad (5)$$

$$x_i^L \leq x_i \leq x_i^U, \quad i = 1, \dots, n \quad (6)$$

where $r_{w\max}$ is the allowable upper bound of the ratio r_w , and $r_{t\min}$ is the allowable lower bound of the ratio r_t . x_i^L and x_i^U are the upper and lower bounds of design variables i , respectively. It is noted that if the given blank is successfully drawn into the cups without defects determined by Eq.(4) and Eq.(5), the values of the design variables are considered as optimal values, though L_a may not be the deepest one. Therefore, the optimal solution for the pulsating BPF may not be only one.

5.2. Optimization results

The SAO method using RBF network is adopted to perform design optimization. In the optimizing process, at first, the response surface of the objective and constraint functions in terms of design variables, is constructed and optimized based on the numerical simulation results of a number of sampling design points. The optimal solution of the response surface is then added as a new sampling design point to improve the local approximation accuracy, and several new sampling points around the unexplored region in the design space are also added to improve global approximation accuracy. At last, the response surface is reconstructed and optimized to get a better optimal solution. This process is repeated until the prescribed terminal criterion is satisfied.

The pulsating BHF applied in the deep drawing process described in this study is optimized. Four parameters of pulsating BHF, F_0 , a , f and ϕ are selected as design variables. The upper and lower bounds of the design variables are given as [0.10, 5.00] for design variable F_0 , [0, 1] for a , [1, 20] for f , and [0, 2π] for ϕ . The $r_{w\max}$ and $r_{t\min}$ are considered as 1.2 and 0.8, respectively.

The optimal values of the design variables are obtained as $F_0 = 4.78$ kN, $a = 0.826$, $f = 4.177$, $\phi = 4.637$, and the optimal pulsating BHF is then calculated by substituting the above four optimal values into Eq.(1), as shown in Figure 7. It is clear that the optimal pulsating BHF curve bypassed both of the wrinkling zone and the tearing zone. The objective value is 29.75 mm, and it is observed that the given blank is drawn successfully into a cup without wrinkling and tearing, as shown in Figure 8. Consequently, it is also may concluded that, a specified larger LDR may be achieved by applying an optimal pulsating BHF during the deep drawing process.

6. Conclusions

This paper proposed a technique to optimize the pulsating BHF to maximize the limiting drawing depth, consequently, to achieve a specified lager LDR. The finite element analysis model was built to simulate deep drawing process of the cylindrical cup using the pulsating BHF, and effects of the pulsating BHF on the drawability were investigated. It's found that the drawability may be improved by applying a proper pulsating BHF. The sequential approximate optimization method was then applied to efficiently search for the optimal pulsating BHF. The proposed optimization technique also can be applied to other optimization

problems of the pulsating BHF under different conditions.

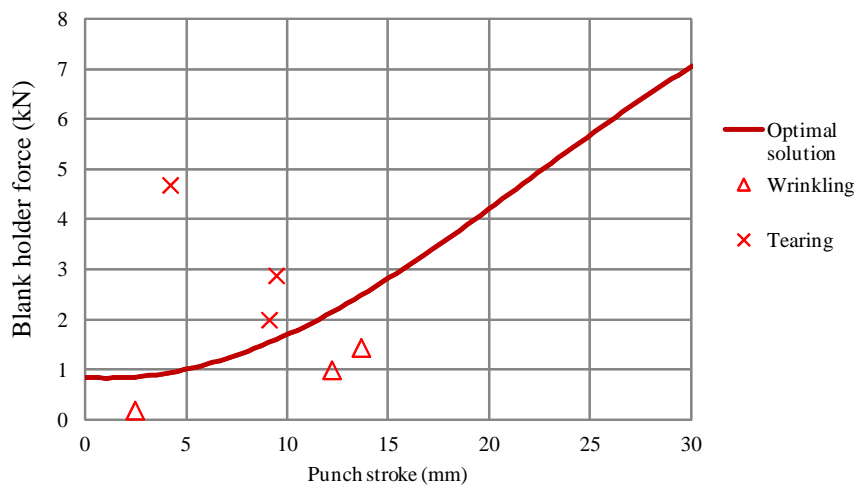


Figure 7: Optimized pulsating BHF

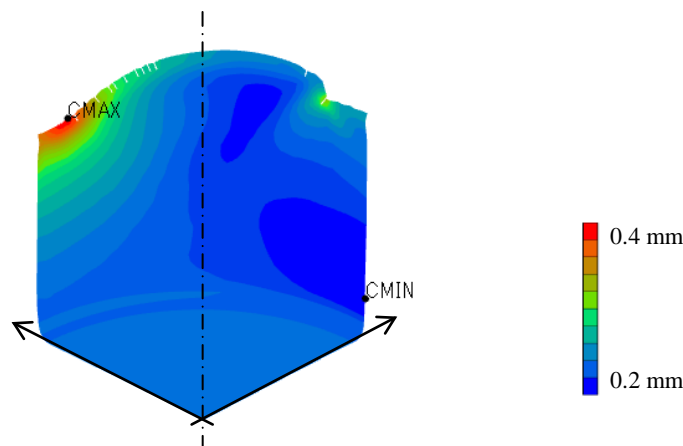


Figure 8: Drawn cup using optimized pulsating BHF

7. References

- [1] S. Y. Chung and H. W. Swift, Cup-drawing from a Flat Blank: Part I. Experimental Investigation, *Proceedings of the Institution of Mechanical Engineers*, 165(1), 199-211, June 1951.
- [2] M.G. El-Sebaie, P.B. Mellor, Plastic instability conditions in the deep-drawing of a circular blank of sheet metal, *International Journal of Mechanical Sciences*, 14(9), Pages 535-540, 1972.
- [3] M. Schünemann, M. A. Ahmetoglu and T. Altan, Prediction of process conditions in drawing and ironing of cans, *Journal of Materials Processing Technology*, 59(1-2), 1-9, 1996.
- [4] A.M Zaky, A.B Nassr, M.G El-Sebaie, Optimum blank shape of cylindrical cups in deep drawing of anisotropic sheet metals, *Journal of Materials Processing Technology*, 76(1-3), 203-211, 1998.
- [5] Cebeli Özek, Muhammet Bal, The effect of die/blank holder and punch radiuses on limit drawing ratio in angular deep-drawing dies, *The International Journal of Advanced Manufacturing Technology*, 40(11-12), 1077-1083, 2009.
- [6] S. M. Mahdavian and Tui Mei Yen Fion, Effect of Punch Geometry in the Deep Drawing Process of Aluminium, *Materials and Manufacturing Processes*, 22(7-8), 2007.
- [7] S. Sezek, V. Savas and B. Aksakal, Effect of Die Radius on Blank Holder Force and Drawing Ratio: A Model and Experimental Investigation, *Materials and Manufacturing Processes*, 25(7), 557-564, 2010.
- [8] I. Dejmali, J. Tirosh, A. Shirizly and L. Rubinsky, On the optimal die curvature in deep drawing processes, *International Journal of Mechanical Sciences*, 44(6), 1245-1258, 2002.
- [9] T. Naka, F. Yoshida, Deep drawability of type 5083 aluminium–magnesium alloy sheet under various

- conditions of temperature and forming speed, *Journal of Materials Processing Technology*, 89–90, 9-23, 1999.
- [10] M.M Moshksar and A. Zamanian, Optimization of the tool geometry in the deep drawing of aluminium, *Journal of Materials Processing Technology*, 72(3), 363-370, 1997.
- [11] J. Han, R. Itoh, S. Nishiyama and K. Yamazaki, Application of structure optimization technique to aluminum beverage bottle design, *Structural and Multidisciplinary Optimization*, 29(4), 304-311, 2005.
- [12] G. Niranjana and U. Chakkingal, Deep drawability of commercial purity aluminum sheets processed by groove pressing, *Journal of Materials Processing Technology*, 210, 1511-1516, 2010.
- [13] K.H.W. Seah and K.S. Lee, The benefits of coating the tools with titanium nitride in the deep drawing of mild steel cups, *Journal of Materials Processing Technology*, 37(1–4), 125-135, 1993.
- [14] M. Y. Demeri, Drawbeads in sheet metal forming, *Journal of Materials Engineering and Performance*, 2(6), 863-866, 1993.
- [15] Y. Q. Shi, Experimental Study of the Small Lubrication Holes on the Die Shoulder on the Formability in Cylindrical Cup Deep-Drawing, *Applied Mechanics and Materials* (Volumes 37-38), 428-431, 2010.
- [16] S. Thiruvardhulan and N.H. Loh, Deep drawing of cylindrical cups with friction-actuated blank holding, *Journal of Materials Processing Technology*, Volume 40, Issues 3–4, January 1994, Pages 343-358
- [17] S. Tommerup and B. Endelt, Experimental verification of a deep drawing tool system for adaptive blank holder pressure distribution, *Journal of Materials Processing Technology*, 212(11), 2529-2540, 2012.
- [18] K. Yamazaki, S. Makino, J. Han and H. Uchida, Earing Minimization with Segmented and Variable Blank Holder Force during Deep Drawing Process for Circular Cup Forming, *11th World Congress on Structural and Multidisciplinary Optimization*, Sydney, Australia, 2015.
- [19] J. Tirosh and P. Konvalina, On the hydrodynamic deep-drawing process, *International Journal of Mechanical Sciences*, Volume 27, Issue 9, 1985, Pages 595-607
- [20] F. Djavanroodi, D. S. Abbasnejad and E. H. Nezami, Deep Drawing of Aluminum Alloys Using a Novel Hydroforming Tooling, *Materials and Manufacturing Processes*, Volume 26, Issue 5, May 2011, pages 796-801
- [21] S.H Zhang, M.R Jensen, J Danckert, K.B Nielsen, D.C Kang and L.H Lang, Analysis of the hydromechanical deep drawing of cylindrical cups, *Journal of Materials Processing Technology*, 103(3), 367-373, 2000.
- [22] Y. Horikoshi, T. Kuboki, M. Murata, K. Matsui and M. Tsubokura, Die design for deep drawing with high-pressured water jet utilizing computer fluid dynamics based on Reynolds' equation, *Journal of Materials Processing Technology*, 218, 99-106, 2015.
- [23] Z. Lai, Quanliang Cao, Bo Zhang, Xiaotao Han, Zhongyu Zhou, Qi Xiong, Xiao Zhang, Qi Chen and Liang Li, Radial Lorentz force augmented deep drawing for large drawing ratio using a novel dual-coil electromagnetic forming system, *Journal of Materials Processing Technology*, In Press, Available online 28 February 2015.
- [24] A. Mostafapur, S. Ahangar and R. Dadkhah, Numerical and experimental investigation of pulsating blankholder effect on drawing of cylindrical part of aluminum alloy in deep drawing process, *The International Journal of Advanced Manufacturing Technology*, 69(5-8), 1113-1121, 2013.
- [25] S. Ali, S. Hinduja, J. Atkinson, P. Ilt and R. Werkhoven, Effect of ultra-low frequency pulsations on tearing during deep drawing of cylindrical cups, *International Journal of Machine Tools and Manufacture*, 48, 558-564, 2008.
- [26] T. Jimma, Y. Kasuga, N. Iwaki, O. Miyazawa, E. Mori, K. Ito and H. Hatano, An application of ultrasonic vibration to the deep drawing process, *Journal of Materials Processing Technology*, 80(81), 406-412, 1998.
- [27] A. Pasierb and A. Wojnar, An experimental investigation of deep drawing and drawing processes of thin walled products with utilization of ultrasonic vibrations, *Journal of Materials Processing Technology*, 34, 489-494, 1992.
- [28] J. Han, K. Yamazaki, R. Itoh and S. Nishiyama, Multi-Objective Optimization of a Two-Piece Aluminum Beverage Bottle Considering Tactile Sensation of Heat and Embossing Formability, *Structural and Multidisciplinary Optimization*, 32(2), 141-151, 2006.
- [29] S. Kitayama, M. Arakawa and K. Yamazaki, Sequential Approximate Optimization using Radial Basis Function network for engineering optimization, *Optimization and Engineering*, 12(4), 535-557, 2011.
- [30] S. Kitayama, K. Kita and K. Yamazaki, Optimization of variable blank holder force trajectory by sequential approximate optimization with RBF network, *Journal of Advanced Manufacturing Technology*, 61(9-12): 1067-1083, 2012.
- [31] S. Kitayama, S. Huang and K. Yamazaki, Optimization of variable blank holder force trajectory for spring back reduction via sequential approximate optimization with radial basis function network, *Structural and Multidisciplinary Optimization*, 47(2): 289-300, 2013.